

Application of Laboratory Based Cone Beam X-ray CT Techniques to Metallurgical Study

Tomohiro NISHIURA* Mitsuharu YONEMURA

Abstract

X-ray computed tomography (CT) is one of the nondestructive visualizing methods which can be observed cross-sections of a physical object. The spatial resolution of the conventional CT equipment has been enhanced remarkably by improving performance of X-ray source and detector which are primary components of a CT scanner. Three dimensional (3D) configuration analysis for the various materials is facilitated by improving the image reconstruction processing speed and easily displaying of 3D shapes. As examples of the laboratory based X-ray CT application to steel & alloy, the 3D analysis of creep voids in the high chromium ferritic steel and precipitates in the nickel based model alloy are described. The laboratory based X-ray CT is also powerful technique for the 3D microstructure analysis.

1. Introduction

The mechanical properties and the deterioration mechanism of steel materials widely employed in automobiles, ships and social infrastructures such as bridges are closely related to their microstructures¹⁾ and its changes. To furnish materials with excellent functions and properties such as strength, ductility and toughness, it is important to control the microstructure that constitutes the crystal structure, lattice defects, grain size and the shape and the volume fraction of the second phase together with its orientation relations and the state of distribution. Since these material factors have hierarchical structures ranging from nanometer to micrometer order in scale, various observation techniques and quantifying techniques are applied to the evaluation of the structures of materials.

Component materials practically used are in the range from millimeter to meter order in scale; therefore, non-homogeneity in metallographic structures often becomes problematic. When structural materials and functional materials are used in a severe environment for a prolonged period, changes in microstructures and or the generation and propagation of cracks occur inside the material before fracture. Therefore, from the viewpoints of reliability and safety, clarification of the fracture phenomena and mechanism is important. As tools for observing the complicated microstructures, and as techniques for analyzing spatial aspects such as three-dimensional (3D) morphology and precipitates distribution, 3D measurement and visualizing techniques attracts attention in many fields.

One of the 3D microstructure analysis is the serial sectioning.²⁾ In this method, the surface layer of a test sample is removed by surface polishing and or fine machining by focused ion beam (FIB), and the two-dimensional image is observed by a microscope. Polishing and observation are repeated to form multiple images that are acquired in the normal direction of the observed plane. A 3D reconstructed data consists of stack of these images.²⁾ And, for example, the three-dimensional atom probe (3DAP) technique is able to visualize the spatial positions of the component elements in a microscopic region of a needle-like sample with the atomic level resolution.³⁾ The transmission electron microscope (TEM) enables the observation of lattice defects such as dislocation with the nanometer resolution and it is excellent in extracting the local crystallographic orientation. As a method for 3D observation by TEM, the stereoscopic observation technique⁴⁾ and computed tomography (CT) have also been developed.^{5,6)}

However, in the case of the above mentioned destructive observation and analysis technique, there exist problems of limited image resolution in the direction normal to the observation plane, and special techniques are needed for preparing samples. In the TEM observation, there also exists the problem of sample size limitation as the power of an electron beam transmitted for materials is not high. The nondestructive observation technique that employs an X-ray probe having high permeability of substances⁷⁾ is one of the 3D imaging techniques. The problem can be solved by X-ray imaging methods.

The X-ray computed tomography scan⁸⁻¹⁰⁾ is based on the image

* Researcher, Dr. Eng., Fundamental Metallurgy Research Lab., Advanced Technology Research Laboratories
1-8 Fuso-cho, Amagasaki, Hyogo Pref. 660-0891

reconstruction from the projection image by radiation in various directions. The first commercial X-ray CT scanner was developed in the early 1970s by EMI and it remains a popular diagnostic imaging technique in the medical field nowadays.^{9,10} In the industrial field, the X-ray CT technique is applied to detect the internal defects in metallic products, taking advantage of its nondestructive nature. The X-ray linear attenuation coefficients of metallic materials are higher than that of human body tissue; therefore, it is difficult for X-ray to penetrate metallic objects. Thus, the observation of micro-scale material structures is usually performed with synchrotron radiation, and in-situ observation is also being attempted.^{8,11}

In recent years, owing to the development of techniques such as the minimization of X-ray source size and the improvement of X-ray imaging detector performance, laboratory based CT instruments having the sub-micrometer spatial resolution are now commercially available.^{8,9} Since opportunity restrictions of the laboratory based X-ray CT measurement are small, laboratory based X-ray CT will become a more effective experimental technique in materials science with the improvement of spatial resolution. In this report, as an example of the application to metallic materials of the most advanced laboratory based cone beam X-ray CT apparatus having the submicrometer spatial resolution, the result of the 3D analysis of creep voids in a creep ruptured specimen of high chromium (Cr) ferritic steel and the result of the observation of the creep voids and the precipitated phase of a nickel (Ni) based model alloy are introduced.

2. Three-dimensional Imaging Technique Using X-ray Probe

The X-ray imaging technique utilizes the transmitted X-ray intensity distribution obtained in the detector, the refracted X-ray and the diffraction patterns. In the general X-ray CT, reconstructed images are obtained by taking advantage of the contrast developed by the difference in the linear attenuation coefficients, transmission images taken from various angles are back-projection-processed, and three-dimensional data are constructed by building-up each cross section image.

Although the refractive index of all materials is close to 1, the refraction phenomenon takes place. Particularly in the region of hard X-rays, the effect of phase difference is large and in the case of objects with low atomic number such as macromolecule, carbon fiber, and in the case of objects with low attenuation contrast, the phase contrast images are enabled.¹² Furthermore, with the use of high brightness, monochromatic, coherent synchrotron radiation for the X-ray source, micro CT technique with the resolution of about 1 micrometer order has been developed. The nano scale CT technique has also been developed. To utilize this imaging, it is common to use X-ray focusing optics to condense the X-ray beam on the object and then to use optics to produce an enlarged image of the object on the detector.^{13,14}

As a technique to determine the crystal orientation on the surface region of a polycrystalline material, identification of crystal orientation by analyzing the diffraction pattern developed by Electron Back Scatter Diffraction (EBSD) is widely executed. As a technique to acquire a 3D crystal orientation mapping of a polycrystalline material using an X-ray with a high penetration power, a technique termed the Three-Dimensional X-ray Diffraction Microscopy (3DXRD)^{8,15} is enabled. This is a technique of acquiring a 3D crystallographic orientation mapping wherein a monochromatic X-ray beam is radiated onto a millimeter sized sample while the sample is

being turned and the diffraction pattern is recorded by a two-dimensional detector, and then the grains are characterized layer by layer. In addition to general X-ray absorption contrast CT, there is Diffraction Contrast Tomography (DCT)¹⁶ that visualizes the 3D configuration of crystal grains by utilizing the information of the position where the crystal grains which satisfy the diffraction condition and the information of the change in absorption contrast.

The Differential Aperture X-ray Microscopy (DAXM) technique¹⁷ is a technique in which a monochromatic or a polychromatic X-ray is concentrated to a beam of submicrometer order diameter by a Kirkpatrick-Baez type reflecting mirror and radiated onto a sample. A Laue diffraction pattern is acquired by a two-dimensional detector. A platinum wire 50 micrometers in diameter scans the sample at the distance of several hundred micrometers above the sample in parallel to the sample surface. By measuring the diffraction pattern intercepted by the platinum wire and identifying the crystalline region that satisfies the diffraction conditions, three-dimensional configuration and the crystalline orientations of a polycrystalline material are determined.

X-ray diffraction microscopy has also been developed¹⁸, wherein the X-ray diffraction pattern of an object is measured and the phase of the diffraction wave is retrieved by computation and images are reconstructed. Noteworthy is the ptychography. This technique utilizes the Coherent Diffractive Imaging (CDI) technique in which, by repeated computations, the information about a sample is acquired from the two-dimensional diffraction intensity data of a sample radiated by a coherent X-ray without using lenses. This technique enhances the phase retrieval accuracy remarkably by utilizing the information of the regions obtained by overlap scanning.¹⁹ Two-dimensional and three-dimensional mappings of not only the configuration images, but also those of strain distribution and stress distribution enabled. The CDI technique provides gray scale value and the identification of elements is impossible. However, by measuring the X-ray fluorescence (XRF) simultaneously, element mapping in observation space is enabled.

Furthermore, even for laboratory based X-ray CT, a group from the Argonne National Laboratory has developed an apparatus which unites the high brightness source manufactured by Rigaku Corporation and the CT technology owned by Carl Zeiss AG, and has realized an apparatus with the spatial resolution of 0.15 micrometer order for the field of vision of 65 micrometers by using a CCD of 1024×1024 pixels.²⁰ The spatial resolution is enhanced further depending on the size of the field of vision. There are several researches using ptychography and in-situ measurement, and regardless of whether the research is laboratory based, or the types of synchrotron radiation, individual research organizations design the fields of temperature and or stress. In particular, several observations of kinetic phenomenon like phase transformation behaviors are being conducted.

On the other hand, the research on metals and ceramics using laboratory based X-ray CT apparatus, has been promoted extensively since the 1980s. However, the spatial resolution power was limited to about several hundred micrometers order.¹⁰ When the resolution was improved to about 1 micrometer order in the field of iron and steel, in the three-dimensional analysis of coke, the structural change in microstructures and voids in coke could be observed in a nondestructive manner based on the CT images before and after the reaction, and the technique has attracted attention as a practical technique.²¹ Currently, even in the laboratory based X-ray CT apparatus, the special resolution has been improved to submicrometer

order, and owing to the improved performance in hardware such as high intensity X-ray source, detector, etc., and owing to the speeding up of the reconstructing processing and the evolution of software for three-dimensional displaying, system generality has been enhanced greatly and application of metallic materials has progressed remarkably. In common with many other science fields, the remarkable progress of computers has improved the usefulness of 3D data analysis of objects in this field.

3. Measurement Technique

The laboratory based X-ray CT apparatus used in the measurement example that is described hereafter consists of a cone beam optical system with a few micrometer X-ray spots size as shown in Fig. 1. When the distance between the X-ray source and the sample is taken as a and the distance between the sample and the detector as b , the change in transmitted X-ray intensity is projected on the detector enlarged by $(1+b/a)$ geometrically. The projection is recorded by the light conversion type detector in the form of 16-bit grey scale data. The sample is turned and each projection is recorded.

When photographing an ordinary absorption contrast image, since the incoming radiation X-ray is attenuated by air, from the viewpoint of measuring time, a shorter distance between the X-ray source and the sample is desirable. However, if a photograph is taken with sufficient distances between the X-ray source and the sample and between the sample and the detector, the slight difference in refraction (phase) of the X-ray that takes place at the boundaries between different materials in the sample can be emphasized as a contrast on the absorption contrast image. The projection data is image-processed like filter processing and reconstructed to provide 3D volume data. In this research, Avizo 9 of FEI Corporation was used as the three-dimensional data for visualizing and analysis software.

4. Application of Laboratory Based X-ray CT Technique to Metallic Material

4.1 Visualization of voids in high Cr ferritic steel specimen after creep rupture test

In this section, as an example of measuring a metallic material by laboratory based X-ray CT apparatus, the visualization of the creep voids of 9 mass% Cr ferritic steel that ruptured in a creep test at high temperature is introduced. In the laboratory based X-ray CT technique, voids above 1 micrometer are observable. Figure 2 shows an outlook view of a test piece near the rupture surface of creep ruptured 9 mass% Cr steel and the magnified reconstructed image of the measured region indicated with a red line in Fig. 2(a). The measuring condition is: 95 kV, source-sample distance: 21 mm and sample-detector distance: 21 mm. Furthermore, the creep test direction was exerted in the upward and downward directions on the paper and the creep void region is displayed, being distinguished

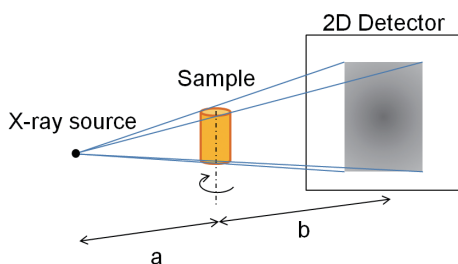


Fig. 1 Schematic of the laboratory based X-ray CT experimental set-up

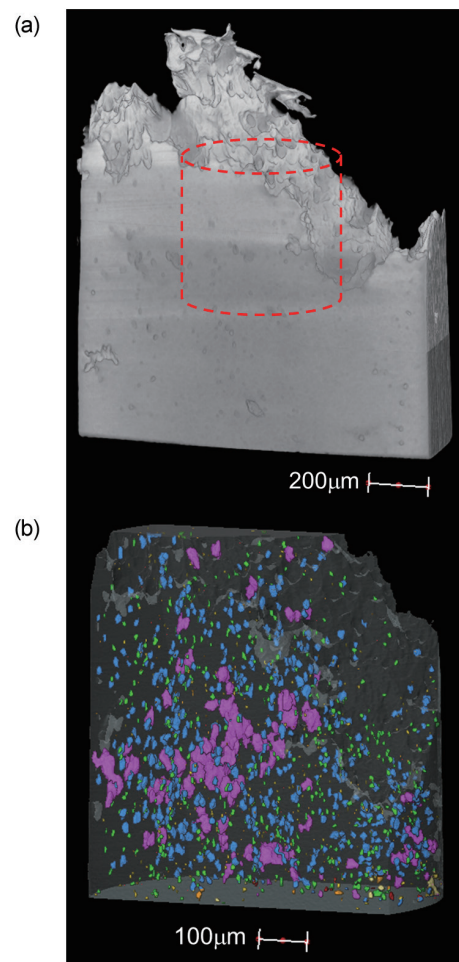


Fig. 2 3D views of a tip of the ruptured 9 mass% Cr steel sample

depending on void size.

Figure 3 shows the reconstructed image taken at 2 mm away from the rupture surface on the tip. Fig. 3(a) shows the perspective image of the sample and the void region. Fig. 3(b) is the image magnified for measuring the region shown with a red line in Fig. 3(a). In the reconstructed volume, the voxel size is 0.68 micrometers. There's a trend of decrease in the number of voids of 30 micrometer³ or above as compared to the voids in the region near the tip. In Fig. 4, the histogram of the volume on the surface of 5 mm away from the rupture surface is shown with other results measured in the same manner. Near the rupture surface, relatively large voids are observed that are developed by joining them together. In the vicinity of the rupture surface of the ruptured specimen, the true stress increases due to necking; therefore, increase in void size caused by stress is considered.

4.2 Visualization of microstructure of Ni based model alloy after creep test

As an example of the three-dimensional analysis of a precipitation phase, an example of measurement of creep test specimen of Ni based model alloy^{22, 23)} is introduced. The creep test was conducted under the condition of 850°C and 100 MPa, using a round bar test piece of 25 mm in gauge length and 6 mm in diameter of the parallel body. The measuring condition is: 80 kV, source-sample distance: 12 mm and sample-detector distance: 70 mm.

Figure 5 shows the back scattered electron compositional

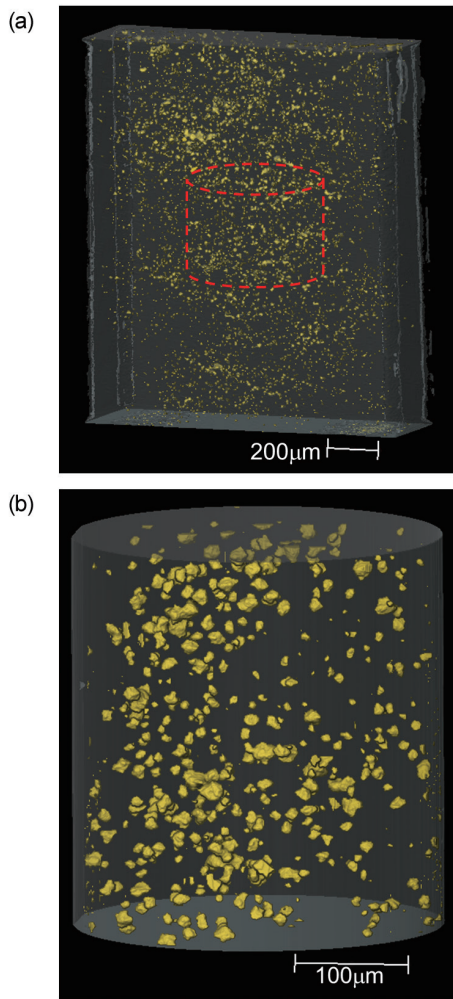


Fig. 3 3D views of 2 mm away from the ruptured sample of 9 mass% Cr steel

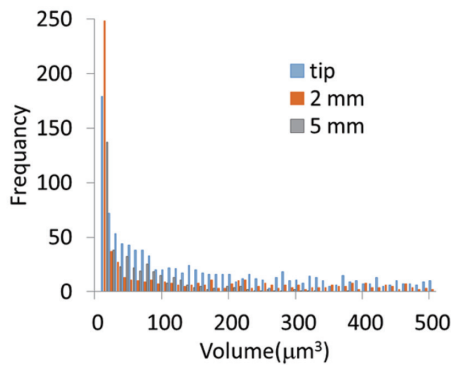


Fig. 4 Histogram of the volume of voids

images of the initial Ni based model alloy and the ruptured Ni based model alloy taken by a scanning electron microscope (SEM). The initial microstructure of the sample consists of mainly the γ' phase, a fine coherent precipitated phase in the FCC parent phase, and the Laves phase at the grain boundaries. On the other hand, as shown in Fig. 5(b), the microstructure after creep rupture consists of the fine γ' phase, a fine coherent precipitate phase in the FCC parent γ phase,

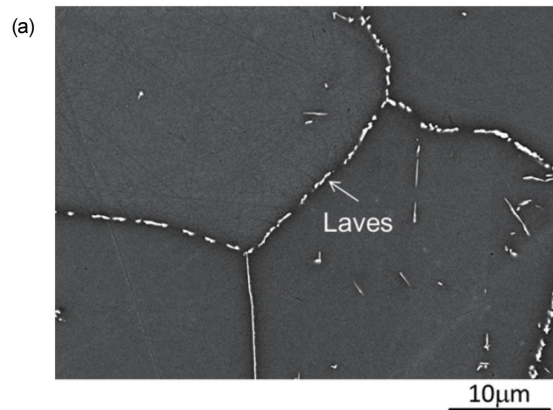


Fig. 5(a) SEM compositional image of the initial Ni based model alloy

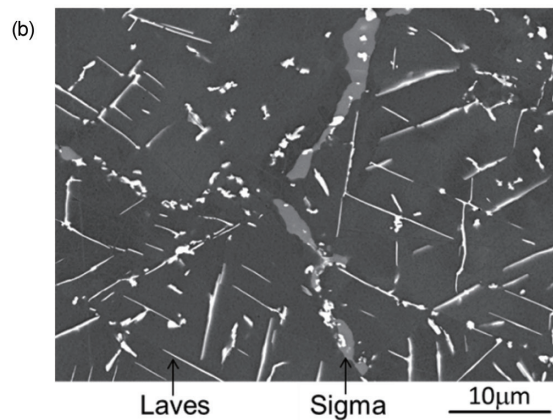


Fig. 5(b) SEM compositional image of the ruptured Ni based model alloy

the Laves phase at the grain boundaries (white contrast) and the σ phase (light grey contrast). Along with the progress of creep, the Laves phase at the grain boundaries changes to the σ phase and the acicular type Laves phase grows in grains.²²⁾ This type of microstructure was observed three-dimensionally by X-ray CT. The CT measuring condition is: 80 kV, source-sample distance: 12 mm and sample-detector distance: 70 mm. By the geometrical magnification in the optical system and by the magnification by means of an object lens, the voxel size of the reconstructed volume is 0.97 micrometers.

First, in Fig. 6, the results of the calculation of mass attenuation coefficients of major phases of sample materials with respect to X-ray photon energy are shown. In the calculation, the typical compositions of the γ phase of Ni-20 mass% Cr, the γ' phase of Ni₃(Al, Ti), the Laves phase of Fe₂W and the σ phase of Fe-50 mass% Cr were assumed and the mass attenuation coefficient of the respective element was based on the data of the National Institute of Standards and Technology (NIST)²⁴⁾. The calculation result indicates no remarkable difference in the mass attenuation coefficients between that of the γ phase and that of the γ' phase of this sample. However, since there are differences in the coefficients between those of the Laves phase and the σ phase and those of the γ phase and the γ' phase, identification of the phase with the contrast in X-ray absorption is possible. The linear attenuation coefficient that is the multiplication of the mass attenuation coefficient by the density of the respective phase also follows a similar trend.

Figure 7(a) shows the reconstructed image of the vertical sec-

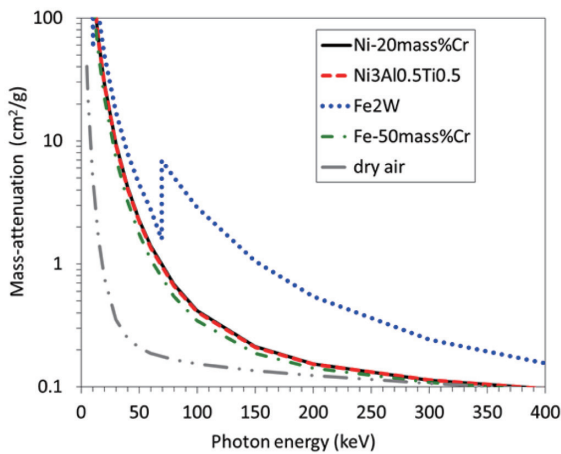


Fig. 6 X-ray mass attenuation coefficients as a function of X-ray energy for materials of Ni based model alloy

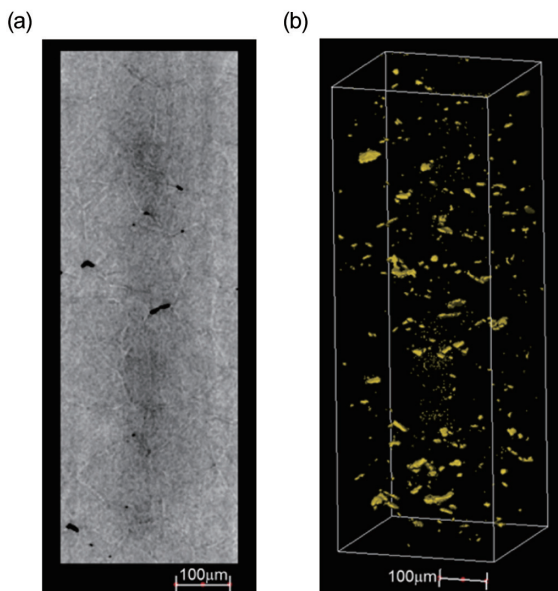


Fig. 7 Vertical CT slice and 3D view of voids in the Ni based model alloy after interrupted creep testing

tion of the sample taken at the center of the test piece after the interruption in the process of accelerating creep (creep elongation, 8%). The creep test stress is exerted in the upward and downward directions on the paper. The dark contrast regions show creep void regions. The slightly bright contrast is the Laves phase at grain boundaries or the σ phase judging from its correspondence to the result of the observation by SEM. The fine Laves phase within a grain is in the acicular state, and under this CT condition, since the size of the acicular microstructure in the short-axis direction is smaller than the resolution (voxel size) of the reconstructed image, the acicular microstructure is displayed in a ripple-like pattern on the reconstructed image and not clearly recognizable. Furthermore, since the fine γ' phase within a grain is smaller than the spatial resolution, the phase is displayed in ripple-like pattern contrast. Figure 7(b) shows a 3D image with creep void regions extracted. Creep voids are recognized at triple points and or among the Laves phase particles at the grain boundaries. Growth of voids is considered to take place in the re-

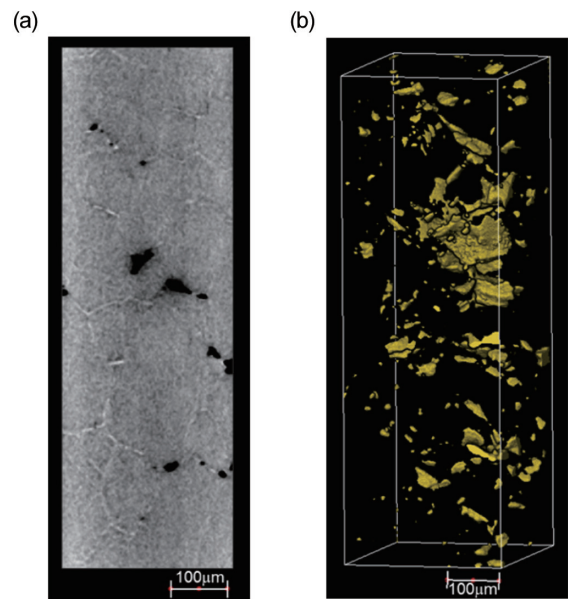


Fig. 8 Vertical CT slice and 3D view of voids in 5 mm away position from the ruptured sample of Ni based model alloy

gions where there is no growth of precipitates hindered by the coarsening of adjacent precipitates at the grain boundaries.

Figure 8(a) shows the vertical section of the measured and reconstructed 3D image of the sample taken at the position 5 mm away from the rupture surface of the test piece. The test force was exerted in the upward and downward directions on the paper. The CT measuring condition is the same as the abovementioned and the voxel size of the reconstructed image is 0.97 micrometers. Corresponding to the result of observation by SEM, the bright network pattern contrast regions show the Laves phase and the regions with different degrees of brightness existing among the Laves phase show the σ phase. In Fig. 8(b), a 3D image drawn up with extracted void regions is shown. The void size is larger than that in the test piece with interrupted creep shown in Fig. 7, and the voids are displayed in a plane-like form. The creep voids are formed and developed at triple points and among the Laves phase particles at the grain boundaries; and at the boundaries with the σ phase, the development of cracks along the grain boundaries is considered.

Thus, laboratory based X-ray CT apparatus enables 3D observation that provides very important information for the analysis of microstructure such as for identifying precipitates, void formation sites, etc.

5. Conclusion

As an example of applying the X-ray CT technique, one of the nondestructive visualization techniques, to the research on metallic materials, the result of three-dimensional analysis of creep void of high Cr ferritic steel and the result of measurement of the creep void and the precipitate phase of Ni based model alloy, both acquired by using the laboratory based X-ray CT apparatus having the spatial resolution of submicrometer order, were introduced. This technique is a powerful tool for observing the microstructures of metallic materials, and furthermore, the technique is expected to contribute to the clarification of phase transformation phenomena and the designing of new materials by combining other observation technologies. With the use of a large-scale facility employing X-ray free electron

laser, challenging technologies are being developed, such as observation by using ptychography in the disintegration process of a material within femto second time order before being damaged. Hereafter, owing to the upgrading of the third-generation synchrotron radiation facility, increase in the research on metals applying sophisticated imaging techniques is expected. We attempt to develop a 3D microstructure analysis technique which combines laboratory based X-ray CT technique with advanced ptychography, based on the international technology trends.

Acknowledgements

We would like to express our sincere appreciation and gratitude to Professor Dorte Juul Jensen, Dr. Søren Fæster and Dr. Yubin Zhang of the Technical University of Denmark for their help and encouragement.

References

- 1) Nishizawa, T.: Mikurososhiki no netsurikigaku [Thermodynamics of Microstructure]. Sendai, The Japan Institute of Metals and Materials, 2005, p.4
- 2) Enomoto, M.: Tetsu-to-Hagané. 90 (4), 183 (2004)
- 3) Takahashi, J. et al.: Shinnittetsu Giho. (390), 20 (2010)
- 4) Tanji, T. et al.: Journal of Electron Microscopy. 54, 215 (2005)
- 5) Koster, A. J. et al.: J. Phys. Chem. B. 104 (40), 9368 (2000)
- 6) Liu, H. H. et al.: Science. 332, 833 (2011)
- 7) Cullty, B. D. (author), Matsumura, G. (translation): Cully X-sen kaisetsu yoron [Elements of X-ray Diffraction]. Tokyo, Agneshofu-sha Inc., 2009, p.459
- 8) Maire, E., Withers, P. J.: International Materials Reviews. 59 (1), 1 (2014)
- 9) Hirao, Y.: Historical Development of X-Ray Computed Tomography for Medical Use. Center of the History of Japanese Industrial Technologies, 2008. <http://sts.kahaku.go.jp/diversity/document/system/pdf/045.pdf>
- 10) Taguchi, I.: Bulletin of the Japan Institute of Metals. 22 (12), 1017 (1983)
- 11) Gussone, J. et al.: Materials Science and Engineering A. 612, 102 (2014)
- 12) Momose, A.: J. Jpn. Soc. Synchrotron Radiation Res. 10 (3), 273 (1997)
- 13) Tanaka, K. et al.: Hoshako niyoru oryoku to hizumi no hyoka [Evaluation of Stress and Strain by Synchrotron Radiation]. Tokyo, Yokendo Inc., 2009, p.28
- 14) Toda, H. et al.: Kenbikyo [Microscopy]. 44 (3), 199 (2009)
- 15) Nielsen, S. F. et al.: Materials Science and Engineering A. 319–321, 179 (2001)
- 16) Ludwig, W. et al.: J. Appl. Cryst. 41, 302 (2008)
- 17) Yang, W. et al.: Micron. 35, 431 (2004)
- 18) Nishino, Y.: Kenbikyo [Microscopy]. 44 (1), 24 (2009)
- 19) Rodenburg, J. M. et al.: PRL 98. 034801 (2007)
- 20) Patterson, B. M. et al.: Materials Characterization. 95, 18 (2014)
- 21) Yamamoto, Y. et al.: Tetsu-to-Hagané. 95 (2), 103 (2009)
- 22) Yonemura, M. et al.: 12th Inter. Conf. Creep and Fracture of Engineering Materials and Structures. A45, (2012)
- 23) Yonemura, M. et al.: Metallurgical and Materials Transactions A. 47 (4), 1898 (2016)
- 24) NIST XCOM web site: <http://www.nist.gov/pml/data/xcom/index.cfm>



Tomohiro NISHIURA
Researcher, Dr. Eng.
Fundamental Metallurgy Research Lab.
Advanced Technology Research Laboratories
1-8 Fuso-cho, Amagasaki, Hyogo Pref. 660-0891



Mitsuharu YONEMURA
Senior Researcher, Dr. Eng.
Fundamental Metallurgy Research Lab.
Advanced Technology Research Laboratories